Micron 120 (2019) 96–103

Contents lists available at ScienceDirect

Micron

journal homepage: www.elsevier.com/locate/micron

The effects of encapsulation on damage to molecules by electron radiation

Stephen T. Skowron, Sarah L. Roberts, Andrei N. Khlobystov, Elena Besley*

School of Chemistry, University of Nottingham, University Park, Nottingham, NG7 2RD, UK

ARTICLE INFO

Keywords:
Electron microscopy
Radiation damage
Encapsulation
Low dimensional materials

ABSTRACT

Encapsulation of materials imaged by high resolution transmission electron microscopy presents a promising route to the reduction of sample degradation, both independently and in combination with other traditional solutions to controlling radiation damage. In bulk crystals, the main effect of encapsulation (or coating) is the elimination of diffusion routes of beam-induced radical species, enhancing recombination rates and acting to limit overall damage. Moving from bulk to low dimensional materials has significant effects on the nature of damage under the electron beam. We consider the major changes in mechanisms of damage of low dimensional materials by separating the effects of dimensional reduction from the effects of encapsulation. An effect of confinement is discussed using a model example of coronene molecules encapsulated inside single walled carbon nanotubes as determined from molecular dynamics simulations calculating the threshold energy required for hydrogen atom dissociation. The same model system is used to estimate the rate at which the nanotube can dissipate excess thermal energy above room temperature by acting as a thermal sink.

1. Introduction

In modern aberration-corrected high-resolution transmission electron microscopy (TEM) the spatial resolution achievable is sufficient to image the position of individual atoms, in principle presenting the ultimate tool for precise characterisation of material structures. As a result, TEM has found a wide array of applications in a range of diverse systems, including biological structures (Murata and Wolf, 2018), polymers (Libera and Egerton, 2010), metal-organic frameworks (Wiktor et al., 2017), and low dimensional nanomaterials (Robertson and Warner, 2013). However, the use of highly energetic electrons inevitably results in the deposition of energy into the system being studied, often leading to structural degradation of the materials being observed. Although this is increasingly being used as an intentional external stimulus driving targeted structural modification

(Hudak et al., 2018; Skowron et al., 2017; Susi et al., 2017; Zhao et al., 2018), for the overwhelming use case of TEM – structural characterisation – this is an unwanted side-effect of the technique that interferes with the determination of intrinsic material structures and properties. For many systems, the limiting factor determining the information that can be obtained from TEM imaging is therefore no longer the spatial resolution of the microscope, but sample degradation under the harsh conditions of the electron beam.

Various 'encapsulation' techniques have been used over the years in order to provide some form of protection from electron radiation. Although we will be primarily considering organic molecules encapsulated in carbon nanomaterials, most of the general principles discussed are independent of the precise nature of the system and are more widely applicable, for example to confinement within ice (relevant to cryo-electron microscopy) and coatings with metal atoms such as gold. Similarly, we will use examples from other systems such as continuous solid nanomaterials in order to demonstrate effects in cases where there is little experimental evidence for specifically molecular systems.

We will begin with a consideration of the primary protective effect of encapsulation of bulk organic crystals in Section 2. In this section, we review quantitative historical investigations in order to introduce a framework for understanding the main effect of encapsulation: the 'cage effect' which limits diffusion and enhances recombination rates of reactive species created by the beam.

The most effective modern methods for imaging individual molecules with TEM involve preparing samples that are low-dimensional, for example via the deposition of single molecules on atomically thin substrates (Markevich et al., 2016; Meyer et al., 2008) or the preparation of one dimensional 'molecular stacks' inside nanotubes (Chamberlain et al., 2017; Liu et al., 2007). Many of these techniques effectively utilise some form of coating or encapsulation in order to achieve the reduction in dimensionality from the bulk molecular crystal. As both of these changes in the nature of the sample being studied have large implications for stability under electron radiation, in

* Corresponding author.
E-mail address: Elena.Besley@nottingham.ac.uk (E. Besley).

https://doi.org/10.1016/j.micron.2019.02.007
Received 26 January 2019; Received in revised form 16 February 2019; Accepted 19 February 2019
Available online 21 February 2019

Section 3 we decouple the effects of low dimensionality and encapsulation by explicitly considering the effects of moving from 3D bulk materials to 2D or 1D nanomaterials.

Section 4 considers the main effects (protective and otherwise) of encapsulation of low dimensional materials, which can be considered to arise from two major aspects of encapsulation: confinement and the introduction of sinks of heat and charge. Results from classical simulations using a model system are presented for two of the mechanisms discussed, in order to quantify their effect. Encapsulating surfaces are shown to slightly increase damage rates by providing an attractive potential as compared to the vacuum, and the ability of protecting surfaces to act as heat sinks is investigated.

2. Protection factors upon encapsulation of three-dimensional organic crystals

The use of protective films to reduce radiation damage and prolong sample lifetimes has a long history in electron microscopy. Important quantitative studies of the nature of this effect were pioneered by J. R. Fryer and colleagues in a series of papers throughout the 1980s (Fryer, 1987, 1984; Fryer et al., 1984; Fryer and Holland, 1984, 1983), following on from earlier observations that carbon, gold and aluminium coatings protected three dimensional molecular crystals imaged in the TEM (Cosslett, 1978). Fryer's series of experiments investigated the degree to which encapsulating amorphous carbon films reduced beam damage to organic crystals, quantified by a 'protection factor'. The protection factor (PF) was initially defined as the relative dose required for the extinction of diffraction peaks in covered and non-covered areas of samples prepared according to the experimental set up shown in Fig. 1a. It is important to note that the PF is distinct from absolute damage rates and is purely a measure of the degree of protection from the beam conferred by the coating.

The decoupling from absolute damage rates enabled measurements of the dependence of the PF on a wide variety of properties, including the chemistry of the molecular species and nature of the coating (Fryer et al., 1984; Fryer and Holland, 1984); the thickness of the crystal and coating layers (Fryer, 1984); and the accelerating voltage and dose rate of the electron beam (Fryer, 1987; Fryer and Holland, 1984). One rationalisation of the variation in PF observed across these different systems is that the main effect of encapsulation is an increase in recombination rates of peripheral atoms broken away by the beam from parent molecules. By limiting the mobility of beam-induced radical species, their diffusion away from their original lattice positions is reduced. The encapsulating carbon film therefore shifts the equilibrium of the reformation reaction towards the stable crystal structure by increasing the partial pressure of the reforming reactants within the solid. This concept is consistent with the generally observed 'cage effect' identified in high resolution imaging studies. Radiation damage is observed to preferentially take place at edges and voids of crystals, and the loss of structure normally occurs more quickly in areas where atoms and fragments can easily diffuse from the crystal matrix. It is therefore not surprising that the elimination of diffusion routes enhances recombination rates, acting to limit overall damage.

The two main lines of evidence for this explanation of sample protection by encapsulation concern the dependence of the PF on the nature of the encapsulated molecules and on the nature of the encapsulating material. Although *absolute* damage rates vary hugely depending on the precise nature of the material being studied under the electron beam, in the above studies the *protection factor* had no observable dependence on the chemical structure, aromaticity, electronic properties, conductivities, or atomic cross-sections of the molecules being irradiated. There was however a strong dependence of the PF on the mass of peripheral atoms in the molecule, with this dependence following the ability of terminating atoms to diffuse away from parent molecules once their bonds have been broken by the electron beam. In this manner, the PF for hydrogenated:chlorinated:brominated molecules was measured to be 3:9:12 (Fryer and Holland, 1983). Similarly, the PF generally showed no dependence on the chemistry of the encapsulating material used, with silicon monoxide coatings providing the same benefit as carbon coatings. A key exception is in the case of encapsulating layers containing terminating halogen atoms, which acted to increase the PF by increasing the partial pressure of free-radical scavengers (Fryer et al., 1984).

The behaviour of organic crystals under electron radiation at low

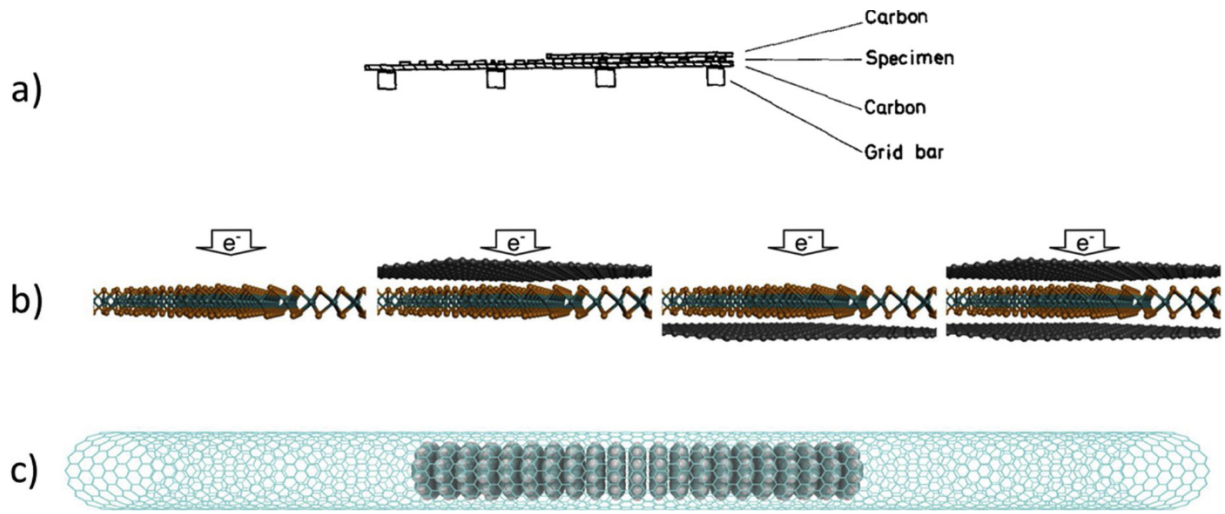

Fig. 1. Representative illustrations of various types of encapsulation discussed in the text. (a) The half covered specimen arrangement used in J. R. Fryer's encapsulation protection factor studies, reprinted from reference (Fryer and Holland, 1983) with permission from Elsevier. By comparing extinction doses from covered and uncovered areas of a single specimen, the effect of the coating was directly measured independently of unintentional variations between different samples (thickness, orientation, etc). (b) The four different graphene/$MoSe_2$ heterostructure configurations used to decouple and limit different electron beam induced damage mechanisms, reprinted from reference (Lehnert et al., 2017), with the permission of AIP Publishing. An advantage of modern 2D materials is that their atomically identical nature removes the need for the half-covering technique, allowing quantitative comparisons between independent samples prepared with different coating geometries. (c) A (19,0) carbon nanotube encapsulating a 'molecular stack' of coronene molecules, one of the model examples used in the calculations in this paper. Coronene is an extensively studied organic molecule in the context of radiation damage experiments and modelling, often used as a prototype molecule representing the class of polyaromatic hydrocarbons.

temperatures also supports these considerations. Low temperatures, particularly below 80 K, were shown to significantly reduce beam-induced damage (as measured by the fading of diffraction patterns), or at least delay the onset of damage for a period known as the 'latent dose' (Fryer et al., 1992). Crystals subjected to a latent dose were observed to subsequently suffer the loss of diffraction peak intensity expected from the total applied dose (including the latent dose) once heated back to room temperature, even if not exposed to significant further electron radiation (Siegel, 1972). This observation can be understood as the beam breaking molecular bonds, with low temperatures preventing subsequent diffusion of fragments, so that damage is only observed upon heating. Once more, the behaviour of species with different atomic structures is very similar, implying the rate-limiting step of damage is diffusion (Fryer et al., 1992).

One important aspect of this framework is that so far there has been no consideration of the mechanism by which the electron beam breaks bonds in molecular species. This has encouraging implications for the versatility of using encapsulation to protect from radiation induced damage as the general principle should be equally applicable to all materials and conditions regardless of which bond dissociation mechanism dominates (radiolysis, direct knock-on processes, etc.). In all cases encapsulation should in principle help to alleviate damage by increasing the rate of healing processes, irrespective of the details of damage occurrence. The effects of encapsulation that are only applicable to specific damage mechanisms are considered in Section 4. Generally the PF increases linearly with decreasing crystal thickness (Fryer, 1984), suggesting that encapsulation techniques should provide superb protection for ultrathin materials, especially in the case of low dimensional nanomaterials.

3. Electron irradiation of low dimensional materials

Unlike the historical studies discussed so far, all of which concerned three dimensional organic crystals encapsulated between amorphous carbon films, modern TEM studies have access to state-of-the-art low dimensional nanomaterials. Carbon supports that are only a single atom thick present ideal surfaces or encapsulating containers for studying molecules with TEM, whether it is graphene as “the ultimate microscope slide” (Bachmatiuk et al., 2015), or single-walled carbon nanotubes (SWNTs) as molecular test-tubes or nanoreactors (Skowron et al., 2017). In both cases, the nanocarbon support does not interfere with imaging, having low contrast with a periodic structure that is easily filtered from images, while it can spatially fix molecules in position to allow them to be studied with TEM. By reducing the dimensionality of the sample and limiting it to 1D or 2D configurations, in conjunction with modern aberration-corrected imaging methods that enable molecular or atomic resolution, the structure and dynamics of individual molecules can be followed in real time and space. Individual reactions under the electron beam can now be directly observed (Chamberlain et al., 2017) instead of measuring extinction doses of diffraction peaks, presenting an ideal route to probing the effects of encapsulation. This approach avoids ambiguities arising from the interpretation of loss of intensity of specific diffraction peaks, provides spatial context to the damage, and enables the observation of intermediate and product species resulting from the electron radiation induced damage (if any).

However, moving from three to lower dimensional materials has significant effects on the nature of damage under the electron beam. When considering damage rates in low dimensional encapsulated systems it is crucial to separate the effects of dimensional reduction from the effects of the encapsulation. In this section, we consider the major changes in mechanisms of damage induced by the electron beam upon reduction of sample dimensionality. This can be considered to have two major aspects which affect damage mechanisms in different ways: ultrathin dimension(s) of the samples and increasing molecular isolation, as summarised in Fig. 2.

3.1. Extreme dimensions

The major difference in beam damage mechanisms in low dimensional systems is due to their extreme thinness in one or more dimensions, which almost entirely eliminates the effects of damage by secondary electrons. In atomically or molecularly thin materials, secondary electrons are emitted predominantly into the vacuum and cannot induce additional damage effectively; given typical mean free paths of secondary electrons, for such a material to interact with a secondary electron, the electron would have to be emitted almost perfectly perpendicular to the primary beam axis. In traditional TEM samples, however, secondary damage mechanisms such as collision cascades typically remain the major component of damage. As an example, it is estimated that approximately 80% of the beam-induced damage to a 100 nm thick sample of poly(methyl methacrylate) PMMA imaged at a 100 keV accelerating voltage is caused by secondary electrons (Wu and Neureuther, 2001).

In most ultra-thin nanomaterials, the stabilising effect due to insignificant damage by secondary electrons is likely to be the overwhelming factor in moving from bulk materials to low dimensional systems. A notable exception to the predicted increase in stability arises when considering strongly insulating materials at very high electron dose rates. In this case, moving to thinner materials can result in a counterintuitive increase in damage rates, as the deposition of primary electrons is eliminated while the emission of secondary electrons is maximised, leading to an increase in the effects of positive charging (Cazaux, 1999). In extreme situations, accumulation of a great amount of positive charge can result in local Coulomb explosions, as observed for boron nitride nanotubes (Wei et al., 2013). The electrostatic damage mechanism is manifested in a dependence on the maximum dose rate of the electron beam used rather than on the total electron dose deposited.

Damage from beam induced temperature increases tend to be strongly sample dependent, ranging from having a negligible effect to being the single factor determining radiation induced damage. The effect of local heating under the electron beam is principally dependent on the radial diffusion of heat (Egerton et al., 2004), and so a reduction in the dimensionality in the beam axis would be expected to have little to no effect on this damage mechanism. However, further dimensional reduction to 1D could in principle limit diffusion of heat and lead to increased damage rates.

3.2. Molecular isolation

Upon reduction of dimensionality, another major effect is to increase the isolation of individual molecules as their number of nearest neighbours are reduced. The primary outcome of molecular isolation is a reduction in damage rates for a range of different damage mechanisms that occur *via* intermolecular reactions, as once the beam ‘activates’ the molecule (by whichever mechanism), the probability of a reaction with a neighbouring molecule is reduced while the relaxation time of the activated molecule remains constant. For example, C_{60} sustains damage under electron radiation primarily by cross-linking to and eventually polymerising with other adjacent C_{60} molecules. By moving from a 3D crystal of bulk fullerene to a 2D monolayer encapsulated between graphene sheets (Mirzayev et al., 2017) to a 1D array encapsulated inside a SWNT (Smith et al., 1998), the number of nearest neighbours is reduced from 12 to 6 to 2, slowing the rate of polymerisation. This principle was noted shortly after the first molecules encapsulated inside nanotubes were imaged (Britz et al., 2004; Koshino et al., 2007).

However, the reduction in number of nearest neighbours also has associated effects that can increase damage rates. In materials where essentially every atom is a surface atom, for example graphene, all direct knock-on damage can be considered as surface 'sputtering', for which the required emission threshold energies (the minimum energy required to eject an atom such that it does not immediately recombine)

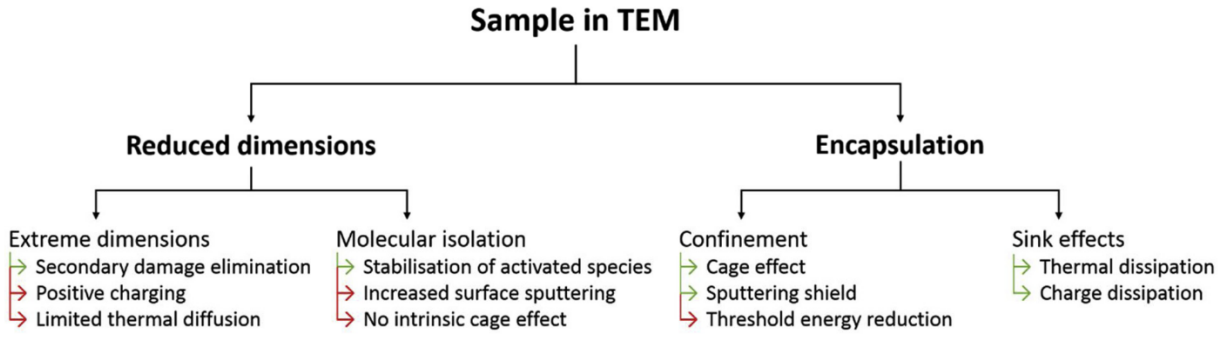

Fig. 2. A summary of the main effects of encapsulation and dimensional reduction discussed in this paper, with the primary effects being either protective (green arrows) or damaging (red arrows) with respect to electron-beam induced damage mechanisms (For interpretation of the references to colour in this figure legend, the reader is referred to the web version of this article).

are lower than in the bulk (Egerton, 2012). In addition, the rates of healing recombination reactions will be lower due to an increased ability of atoms and fragments to diffuse once released, compared to the bulk where the three dimensional nature provides an intrinsic cage effect.

Overall, the exact benefit or otherwise of moving to lower dimensional systems is dependent on the relative importance of the different mechanisms of damage taking place, the chemistry of the molecular species being studied and the nature of the beam (accelerating voltage, electron dose rate, etc). As a general rule, but with certain exceptions as noted above, the increased molecular isolation and elimination of almost all secondary damage mechanisms greatly increases the stability of low dimensional materials under the beam compared to their bulk equivalents.

4. Low dimensional encapsulated materials

In addition to the general protective effects of encapsulation due to the increase in recombination rates and cage effect for three dimensional bulk crystals (as discussed in Section 2), there are several other important consequences of encapsulation, some of which are more relevant to lower dimensional materials. These can be broadly considered to fall under two categories: some, like the cage effect, result from confinement by the encapsulating layers, while others are benefits derived from conducting encapsulating materials acting as sinks to alleviate the build-up of heat or charge.

4.1. Confinement effects

As discussed in Section 3.2, the sputtering of atoms from surfaces occurs more readily than in the bulk, presenting an especially relevant damage mechanism for low dimensional nanomaterials. Coating the exit surface of such materials can help to alleviate this problem by providing a protective 'sacrificial layer' that is preferentially sputtered (Egerton, 2013), while the coating of both entrance and exit surfaces of bulk materials is beneficial. The coating of two-dimensional MoS_2 (Algara-Siller et al., 2013) and $MoSe_2$ (Lehnert et al., 2017) with protective graphene layers in the variety of heterostructure configurations shown in Fig. 1b provided up to a 600-fold reduction in damage rates while enabling the contributions of different damage mechanisms to be decoupled from one another. While coating with a single layer of graphene would be expected to protect from inelastically induced damage mechanisms (as discussed in more detail in Section 4.2), applying this coating to the exit surface of the material rather than the entry surface led to the elimination of an additional 24% of the observed sample damage. This is attributable to the reduction of surface sputtering caused by direct knock-on damage, being the only damage mechanism that should show such a directional dependence on the sample geometry. Notably, 'sandwich' structures in which both sides of the sample were coated with graphene increased the protective ability even further, which may be due to the reduction of atomic diffusion acting to greatly enhance recombination rates and limit damage as discussed in Section 2.

However, the presence of an encapsulating surface surrounding the sample can also in certain cases produce the opposite effect; that is, a slight reduction in atom emission threshold energies and therefore an increase in damage rates. By providing an attractive potential compared to the vacuum via dispersion forces, the energy required from the beam to break a bond is reduced. Fig. 3 demonstrates this effect using a model example of coronene molecules encapsulated inside SWNTs, determined from molecular dynamics simulations calculating the threshold energy required for hydrogen atom dissociation. Simulations were performed using the large-scale atomic/molecular massively parallel simulator (LAMMPS) classical molecular dynamics code

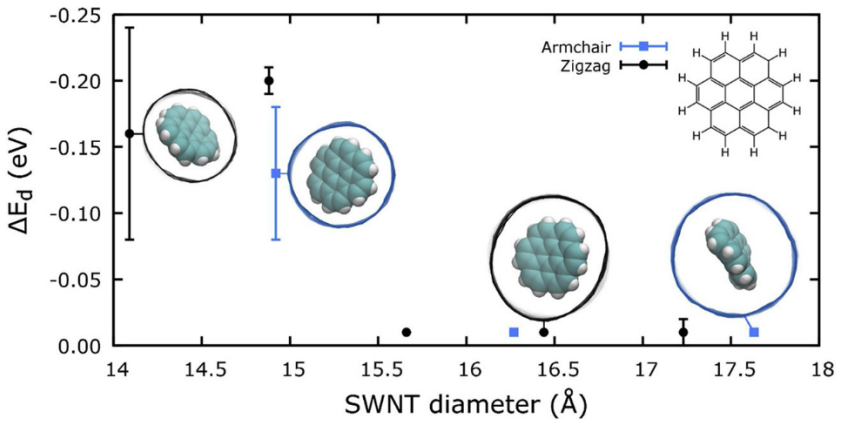

Fig. 3. The mean change in threshold energy (E_d) required for hydrogen dissociation from a nanotube-encapsulated coronene molecule induced by the proximity of the zigzag (black circles and lines) and armchair (blue squares and lines) SWNT walls. The error bars indicate the standard deviation of the variation in ΔE_d dependent on the angle of kinetic energy transfer from the beam. Inset: orthographic projections of the optimised (18, 0), (11, 11), (21, 0), and (13, 13) systems viewed along the tube axis, showing the Van der Waals radii of the coronene atoms in relation to the SWNT walls. Carbon atoms are shown in cyan, hydrogen atoms are shown in white, and the structure of coronene is shown in the top right (For interpretation of the references to colour in this figure legend, the reader is referred to the web version of this article).

(Plimpton, 1995) with the adaptive intermolecular reactive empirical bond order (AIREBO) potential (Stuart et al., 2000). Eight SWNTs were selected to match the diameters of commonly observed experimental nanotubes containing organic molecules (armchair: (11, 11) D = 14.92 Å; (12, 12) D = 16.27 Å; (13, 13) D = 17.63 Å; zigzag: (18, 0) D = 14.09 Å; (19, 0) D = 14.88 Å; (20, 0) D = 15.66 Å; (21, 0) D = 16.44 Å; (22, 0) D = 17.23 Å). A section of nanotube 200 Å long was prepared in the centre of a simulation cell with dimensions of 400 × 400 × 400 $Å^3$ and periodic boundary conditions.

For the threshold energy calculations summarised in Fig. 3, a single coronene molecule was placed in the centre of a nanotube and following a full geometry optimisation of the system each nanotube structure was equilibrated at 300 K for a total of 2 ns using the NVT ensemble and Nosé-Hoover thermostat. Transfer of kinetic energy from the electron beam was modelled by altering the velocity of the primary knock-on hydrogen atom during a single simulation timestep and then propagating the molecular dynamics of the system using the NVE ensemble and a time step of 0.01 fs. The threshold energy for breaking a carbon-hydrogen bond was calculated as the minimum kinetic energy, transferred in such a manner, required to stretch the C–H bond length beyond 1.83 Å, the value above which the bond dissociates with no barrier. Using the same simulation approach, the minimum hydrogen emission threshold energy of a single gas phase coronene molecule with energy transferred directly along the C–H bond is calculated to be 5.65 eV.

Recent results (Chirita et al., 2018) have shown that the specific thermal motion of the atoms involved at the time of the electron impact can alter the threshold energy by up to several eV at room temperature. To avoid these thermal effects and to decouple these results from the angular dependence of the threshold energy – the energy required to break the C–H bond is dependent on the precise angle at which the kinetic energy is transferred to the hydrogen atom – Fig. 3 shows the difference in threshold energy between identical simulations with the only difference being the presence or absence of the encapsulating nanotube, across a range of angles of transferred momentum relative to the molecule and nanotube wall. For each of the eight nanotube encapsulating systems, the energy was transferred in five different directions for hydrogen atoms on the equilibrated coronene structure.

Fig. 3 shows that the threshold energy for hydrogen emission in the presence of the nanotube wall was either less than or equal to the corresponding threshold energy in the gas phase. For very narrow nanotubes that are in close contact with the encapsulated molecules, the threshold energy for breaking terminating carbon-hydrogen bonds can be reduced by up to approximately 0.25 eV, with the exact effect dependent on the precise nanotube chirality and angle of emission relative to the nanotube wall. Above a certain diameter of nanotube the wall is sufficiently far from the breaking bond of the molecule that the threshold energy converges to the vacuum emission threshold energy (this diameter is 15 to 15.5 Å for the coronene molecules), and there is no damaging effect induced by the surrounding surface. This effect will be dependent on the precise system involved and is not universal to all encapsulating/encapsulated materials. The reduction of threshold energy upon encapsulation is relatively minor; it is unlikely to overcome the protective confinement effect of increasing recombination rates but will counteract it by a moderate amount. However, this would be important in cases where direct knock-on effects dominate damage processes, in conditions very close to the damage onset energy, acting to reduce the accelerating voltage at which damage occurs.

The effect of the reduction of displacement threshold energy also occurs when bilayer graphene is exposed to electron radiation. At beam energies and doses in which the atomic structure of monolayer graphene remains pristine, the formation of divacancy defects is observed in bilayer graphene (Zubeltzu et al., 2013). The second layer of graphene enables the creation of divacancies due to the stabilisation of an otherwise unstable intermediate Frenkel pair defect; the additional graphene layer effectively catalyses defect creation and increases damage rates under the electron beam.

4.2. Encapsulating materials as sinks of heat and charge

A major source of electron-beam induced damage, particularly to organic molecules and related 'soft' materials, is due to beam-induced heating. Although this is generally a highly material-dependent damage mechanism and is usually a problem specific to insulating materials, it tends to be the dominating factor in systems in which it occurs and can result in melting or other thermal degradation. Most energy deposited by the electron beam into the sample – by any mechanism, although predominantly by inelastic scattering (electron-electron collisions) – inevitably ends up as thermal energy following relaxation. Coating samples with a conductive material can reduce or entirely eliminate damaging effects due to thermal energy by providing an efficient heat sink. Graphene and carbon nanotubes are among the best candidate materials for acting as thermal sinks – via the use of coatings or encapsulation, respectively – due to their superb thermal conductivities and extreme thinness. Assuming sufficient thermal contact between the material of interest and the coating, local heating due to the electron beam is typically dissipated very quickly, avoiding the problematic build-up of heat over time.

Using a model system, shown in Fig. 1c, we estimate the rate at which such a system can dissipate excess thermal energy above room temperature. A 20 nm long section of (19,0) SWNT containing a stack of 21 coronene molecules separated by 4 Å was optimised, then heated to and equilibrated at 500 K. A single ring of carbon atoms at either end of the nanotube was assigned zero velocity and fixed in position within the simulation box. Three further rings of carbon atoms at each end of the nanotube were included in an NVT ensemble at 300 K, essentially acting as the room temperature heat-sink, while all other atoms were included in an NVE ensemble. The molecular dynamics simulation was propagated for 200 ps whilst the temperature of both the nanotube and the molecular stack were monitored separately, as shown in Fig. 4.

If the nanotube ends are allowed to act as thermal sinks, the SWNT returns to room temperature after approximately 10 ps; the encapsulated molecular stack cools to 300 K via the tube in approximately 100 ps. As the initial system represents much more significant and extensive heating than is typically induced by a single event from the electron beam, this shows sufficiently rapid and efficient heat transfer to render the heating effect of the beam negligible.

Radiolysis, caused by inelastic electron-electron collisions, is the primary damage mechanism in insulating materials such as most organic materials. The formation of charged molecular species following ionisation can lead to destruction of individual molecules and more widespread structural degradation of the sample. In thicker materials the capture of electrons with very low kinetic energy (whether from secondary electrons or, in even thicker materials, slowed primary electrons) leads to dissociative electron attachment (DEA) via the population of antibonding orbitals. In low dimensional and extremely thin nanomaterials, the effect of secondary electrons is negligible (as discussed in Section 3.1) and incident electrons maintain most of the primary kinetic energy, being typically limited to a single interaction during their brief transmission through the sample structure. As a result, for these materials ionisation caused by the emission of core and valence electrons leads to positive charging and subsequent damage. Encapsulation within highly electronically conductive materials such as metals or carbon nanomaterials can protect materials from both of these processes, by providing an efficient transfer of electrons from or to the sample, respectively, and removing excess charge. Notably, the use of gold TEM grids for cryo-electron microscopy (Russo and Passmore, 2014) has in part been driven by the increase in stability due to their excellent conductivity (Russo and Passmore, 2016).

A related but subtly different process can occur from the direct excitation of atomic electrons by inelastic collisions from the beam. Although no charged species are formed, the simultaneous population

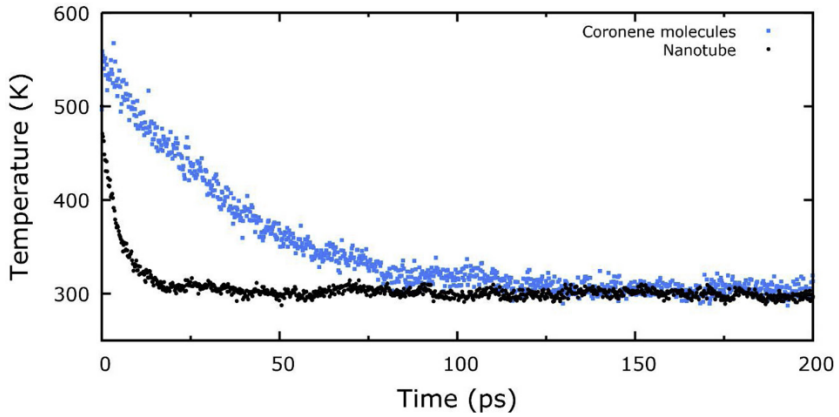

Fig. 4. Time taken for the SWNT and one-dimensional encapsulated stack of coronene molecules (shown in Fig. 1c) to return to room temperature via thermal dissipation through the tube after being heated in our molecular dynamics simulations.

of antibonding orbitals and depletion of bonding orbitals leads to dissociative excitation of molecules. For such processes the role of encapsulation is much less clear than in the case of charged species, and will vary hugely depending on the specific molecules, encapsulating materials, and combinations of the two employed. However, encapsulating materials in electronic contact with such excited states can act to reduce the consequences for molecular damage, for example by enhancing relaxation rates via interactions with delocalised electrons. An additional effect that may have to be taken into consideration is charge transfer between molecular and encapsulating materials, particularly relevant in systems containing strongly electron donating or accepting species. Although the ground state electronic structure can be substantially altered and associated shifts in frontier orbital energies of up to 1 eV have been reported (McSweeney et al., 2016), the consequences for rates of excitation processes leading to damage are unclear.

There are few experimental studies directly measuring the effects of encapsulation on specifically inelastically induced damage, as decoupling the contributions of different damage mechanisms remains challenging. One method employed is the selective graphene 'sandwiching' technique (Algara-Siller et al., 2013; Lehnert et al., 2017) discussed in Section 4.1 and shown in Fig. 1b, which measured the proportion of the reduction in damage from the application of a single layer of graphene that was attributable to protection against radiolysis as 55%–63% of the total damage observed under the electron beam. Even in this case it is unclear whether this damage mechanism is primarily due to charging, excitation, or both processes, and the comparison of MoS_2 and $MoSe_2$ damage rates (Lehnert et al., 2017) raises questions over the interpretation of these results and the understanding of electron radiation induced damage more generally. Further limited evidence for this protective effect lies with the comparative rates of fullerene degradation under the electron beam when encapsulated inside SWNTs of different diameters and degrees of contact with the sample grid (Chuvilin et al., 2010). In general, fullerenes were observed to coalesce at much lower electron doses when encapsulated in wider and freer-standing SWNTs, in which the fullerene-nanotube and nanotube-grid electronic (and thermal) contacts are worse, respectively.

Meanwhile, in contrast to mechanisms involving direct knock-on damage, modelling of these processes also presents difficulties. The beam is able to trigger any feasible electronic excitation process, resulting in many different processes occurring simultaneously, each with associated cross-sections, relaxation times, and propensities to ultimately lead to structural damage. The number of parameters required to accurately model damage under continued electron irradiation therefore quickly skyrockets with system complexity; for example, simply modelling the primary radiolysis products of pure water requires kinetic information for at least 79 different reactions (Schneider et al., 2014). In general, electronic excitation processes occurring under the electron beam and the influence these have on sample stability remain among the most poorly understood aspects of beam-induced damage in TEM.

5. Conclusions

Sample degradation due to radiation damage, in the form of bond breakage and mass loss, occurs under the working conditions of TEM and presents severe limitations for imaging high resolution details of materials. Many of the detrimental effects of radiation damage have been recognised since early developments of the electron microscope (Menter, 1956) but in recent years the problem of radiation damage has been revisited due to its significance in the area of high-resolution imaging of low dimensional materials and molecular samples made of low atomic number elements such as carbon, hydrogen, nitrogen, and oxygen.

As the degree of damage is often dependent on the total acquired electron dose, one approach to overcoming this limitation is to limit the electron dose in the area identified for high-resolution imaging. Hardware developments incorporating the use of direct electron detectors in TEMs present highly promising opportunities for reducing the dose required for image formation by removing inefficient electron-photon conversions (Jin et al., 2008; Mir et al., 2017). Low-dose software such as the Minimal Dose System (MDS) interface can be used to locate an area of interest with a low magnification and to accurately determine the required focus by shifting to an adjacent area thus avoiding pre-exposing the area of interest to high electron dose. Successful integration of this approach when imaging molecular samples can reliably provide high-resolution images prior to the onset of significant damage. The development of more sophisticated low dose imaging modes has aimed to reduce the number of electrons passing through sample, either by effectively spreading the dose through multiple atomically identical species and reconstructing single images – large-area low-dose reconstruction techniques (Meyer et al., 2014) – or by using statistical approaches for the smarter deposition of the dose, for example recent sub-sampling and inpainting methods (Stevens et al., 2018). Alternatively, ultrafast TEM (Zewail and Thomas, 2009) presents a method for forming images before the dose deposited into the material has time to lead to any changes in atomic structure, but this approach greatly reduces the spatial resolution achievable, and the potential of such techniques is fundamentally limited by Coulomb repulsion between electrons in short pulses (Egerton, 2015).

The other main approach to limiting damage is to increase the effective dose that the sample can withstand, either by changing the imaging conditions (tuning the accelerating voltage (Kaiser et al., 2011) or dose rate (Jones et al., 2018) while taking into account the dominant

damage mechanisms taking place) or by altering the sample being studied (for example via isotopic substitution (Chamberlain et al., 2015)). The focus of this paper is on encapsulation techniques, which represent another valuable sample alteration method for achieving increased stability of samples under the electron beam. In some cases (Algara-Siller et al., 2013) encapsulation allows almost the entire elimination of damage, removing it as the limiting factor preventing atomically resolved images. Typical methods employed for controlling radiation damage generally focus on reducing the rate of forward reactions driving the loss of structure (sputtering of atoms, bond breaking etc.). However, recombination ('healing') processes, which involve species displaced by radiation, can also significantly reduce damage to materials. An increase in the rate of reverse reactions is the primary effect of encapsulation, leading to a reduction in sample degradation. This general principle is independent of the nature and mechanisms of radiation damage and is applicable to all materials and imaging conditions thus making encapsulation a versatile and universal method for protection from radiation induced damage.

In low dimensional encapsulated systems, damage rates are also affected by the changes arising from reduced dimensions and molecular isolation, and in the present work these effects are decoupled from the influence of encapsulation on molecular damage under electron radiation. However, the combination of these effects can have a substantial cooperative increase in stability: moving from a 3D crystal to a 1D encapsulated stack of coronene increases the total electron dose that can be withstood by a factor of ~340 (from 1.2×10^4 to 4.1×10^6 e^-/nm^2 (Chamberlain et al., 2015)). Altering the sample chemistry, for example via halogenation in order to benefit from both a reduction in direct knock-on damage and an increase in encapsulation protection factor, can provide an additional factor of ~50, enabling organic molecules to withstand electron doses of 2×10^8 e^-/nm^2 before undergoing any beam induced reactions (Chamberlain et al., 2017). When combined with low dose imaging techniques, this presents a promising methodology for studying the structure and dynamics of individual molecules at atomic resolution for extended periods of time.

Declarations of interest

No competing interests to declare.

References

Algara-Siller, G., Kurasch, S., Sedighi, M., Lehtinen, O., Kaiser, U., 2013. The pristine atomic structure of MoS 2 monolayer protected from electron radiation damage by graphene. Appl. Phys. Lett. 103, 203107. https://doi.org/10.1063/1.4830036.

Bachmatiuk, A., Zhao, J., Gorantla, S.M., Martinez, I.G.G., Wiedermann, J., Lee, C., Eckert, J., Rummeli, M.H., 2015. Low voltage transmission electron microscopy of graphene. Small 11, 515–542. https://doi.org/10.1002/smll.201401804.

Britz, D.A., Khlobystov, A.N., Wang, J., O'Neil, A.S., Poliakoff, M., Ardavan, A., Briggs, G.A.D., 2004. Selective host–guest interaction of single-walled carbon nanotubes with functionalised fullerenes. Chem. Commun. 4, 176–177. https://doi.org/10.1039/B313585C.

Cazaux, J., 1999. Mechanisms of charging in electron spectroscopy. J. Electron Spectros. Relat. Phenomena 105, 155–185. https://doi.org/10.1016/S0368-2048(99)00068-7.

Chamberlain, T.W., Biskupek, J., Skowron, S.T., Bayliss, P.A., Bichoutskaia, E., Kaiser, U., Khlobystov, A.N., 2015. Isotope substitution extends the lifetime of organic molecules in transmission electron microscopy. Small 11, 622–629. https://doi.org/10.1002/smll.201402081.

Chamberlain, T.W., Biskupek, J., Skowron, S.T., Markevich, A.V., Kurasch, S., Reimer, O., Walker, K.E., Rance, G.A., Feng, X., Müllen, K., Turchanin, A., Lebedeva, M.A., Majouga, A.G., Nenajdenko, V.G., Kaiser, U., Besley, E., Khlobystov, A.N., 2017. Stop-frame filming and discovery of reactions at the single-molecule level by transmission electron microscopy. ACS Nano 11, 2509–2520. https://doi.org/10.1021/acsnano.6b08228.

Chirita, A.I., Susi, T., Kotakoski, J., 2018. Influence of temperature on the displacement threshold energy in graphene. Arxiv, 1811.04011.

Chuvilin, A., Khlobystov, A.N., Obergfell, D., Haluska, M., Yang, S., Roth, S., Kaiser, U., 2010. Observations of chemical reactions at the atomic scale: dynamics of metal-mediated fullerene coalescence and nanotube rupture. Angew. Chemie Int. Ed. 49, 193–196. https://doi.org/10.1002/anie.200902243.

Cosslett, V.E., 1978. Radiation damage in the high resolution electron microscopy of biological materials: a review*. J. Microsc. 113, 113–129. https://doi.org/10.1111/j.1365-2818.1978.tb02454.x.

Egerton, R.F., 2012. Mechanisms of radiation damage in beam-sensitive specimens, for TEM accelerating voltages between 10 and 300 kV. Microsc. Res. Tech. 75, 1550–1556. https://doi.org/10.1002/jemt.22099.

Egerton, R.F., 2013. Control of radiation damage in the TEM. Ultramicroscopy 127, 100–108. https://doi.org/10.1016/j.ultramic.2012.07.006.

Egerton, R.F., 2015. Outrun radiation damage with electrons? Adv. Struct. Chem. Imaging 1, 5. https://doi.org/10.1186/s40679-014-0001-3.

Egerton, R.F., Li, P., Malac, M., 2004. Radiation damage in the TEM and SEM. Micron 35, 399–409. https://doi.org/10.1016/j.micron.2004.02.003.

Fryer, J.R., 1984. Radiation damage in organic crystalline films. Ultramicroscopy 14, 227–236. https://doi.org/10.1016/0304-3991(84)90091-3.

Fryer, J., 1987. The effect of dose rate on imaging aromatic organic crystals. Ultramicroscopy 23, 321–327. https://doi.org/10.1016/0304-3991(87)90242-7.

Fryer, J.R., Holland, F., 1983. The reduction of radiation damage in the electron microscope. Ultramicroscopy 11, 67–70. https://doi.org/10.1016/0304-3991(83)90055-4.

Fryer, J.R., Holland, F., 1984. High resolution electron microscopy of molecular crystals. III. Radiation processes at room temperature. Proc. R. Soc. A Math. Phys. Eng. Sci. 393, 353–369. https://doi.org/10.1098/rspa.1984.0062.

Fryer, J.R., McNee, C., Holland, F.M., 1984. The further reduction of radiation damage in the electron microscope. Ultramicroscopy 14, 357–358. https://doi.org/10.1016/0304-3991(84)90221-3.

Fryer, J.R., McConnell, C.H., Zemlin, F., Dorset, D.L., 1992. Effect of temperature on radiation damage to aromatic organic molecules. Ultramicroscopy 40, 163–169. https://doi.org/10.1016/0304-3991(92)90057-Q.

Hudak, B.M., Song, J., Sims, H., Troparevsky, M.C., Humble, T.S., Pantelides, S.T., Snijders, P.C., Lupini, A.R., 2018. Directed atom-by-atom assembly of dopants in silicon. ACS Nano 12, 5873–5879. https://doi.org/10.1021/acsnano.8b02001.

Jin, L., Milazzo, A.-C., Kleinfelder, S., Li, S., Leblanc, P., Duttweiler, F., Bouwer, J.C., Peltier, S.T., Ellisman, M.H., Xuong, N.-H., 2008. Applications of direct detection device in transmission electron microscopy. J. Struct. Biol. 161, 352–358. https://doi.org/10.1016/j.jsb.2007.10.007.

Jones, L., Varambhia, A., Beanland, R., Kepaptsoglou, D., Griffiths, I., Ishizuka, A., Azough, F., Freer, R., Ishizuka, K., Cherns, D., Ramasse, Q.M., Lozano-Perez, S., Nellist, P.D., 2018. Managing dose-, damage- and data-rates in multi-frame spectrum-imaging. Microscopy 67, i98–i113. https://doi.org/10.1093/jmicro/dfx125.

Kaiser, U., Biskupek, J., Meyer, J.C., Leschner, J., Lechner, L., Rose, H., Stöger-Pollach, M., Khlobystov, A.N., Hartel, P., Müller, H., Haider, M., Eyhusen, S., Benner, G., 2011. Transmission electron microscopy at 20kV for imaging and spectroscopy. Ultramicroscopy 111, 1239–1246. https://doi.org/10.1016/j.ultramic.2011.03.012.

Koshino, M., Tanaka, T., Solin, N., Suenaga, K., Isobe, H., Nakamura, E., 2007. Imaging of single organic molecules in motion. Science 80 (316). https://doi.org/10.1126/science.1138690. 853–853.

Lehnert, T., Lehtinen, O., Algara–Siller, G., Kaiser, U., 2017. Electron radiation damage mechanisms in 2D MoSe2. Appl. Phys. Lett. 110, 033106. https://doi.org/10.1063/1.4973809.

Libera, M.R., Egerton, R.F., 2010. Advances in the transmission electron microscopy of polymers. Polym. Rev. 50, 321–339. https://doi.org/10.1080/15583724.2010.493256.

Liu, Z., Yanagi, K., Suenaga, K., Kataura, H., Iijima, S., 2007. Imaging the dynamic behaviour of individual retinal chromophores confined inside carbon nanotubes. Nat. Nanotechnol. 2, 422–425. https://doi.org/10.1038/nnano.2007.187.

Markevich, A., Kurasch, S., Lehtinen, O., Reimer, O., Feng, X., Müllen, K., Turchanin, A., Khlobystov, A.N., Kaiser, U., Besley, E., 2016. Electron beam controlled covalent attachment of small organic molecules to graphene. Nanoscale 8, 2711–2719. https://doi.org/10.1039/C5NR07539D.

McSweeney, R.L., Chamberlain, T.W., Baldoni, M., Lebedeva, M.A., Davies, E.S., Besley, E., Khlobystov, A.N., 2016. Direct measurement of electron transfer in nanoscale host-guest systems: metallocenes in carbon nanotubes. Chem. - A Eur. J. 22, 13540–13549. https://doi.org/10.1002/chem.201602116.

Menter, J.W., 1956. The direct study by electron microscopy of crystal lattices and their imperfections. Proc. R. Soc. A Math. Phys. Eng. Sci. 236, 119–135. https://doi.org/10.1098/rspa.1956.0117.

Meyer, J.C., Girit, C.O., Crommie, M.F., Zettl, A., 2008. Imaging and dynamics of light atoms and molecules on graphene. Nature 454, 319–322. https://doi.org/10.1038/nature07094.

Meyer, J.C., Kotakoski, J., Mangler, C., 2014. Atomic structure from large-area, low-dose exposures of materials: a new route to circumvent radiation damage. Ultramicroscopy 145, 13–21. https://doi.org/10.1016/j.ultramic.2013.11.010.

Mir, J.A., Clough, R., MacInnes, R., Gough, C., Plackett, R., Shipsey, I., Sawada, H., MacLaren, I., Ballabriga, R., Maneuski, D., O'Shea, V., McGrouther, D., Kirkland, A.I., 2017. Characterisation of the Medipix3 detector for 60 and 80 keV electrons. Ultramicroscopy 182, 44–53. https://doi.org/10.1016/j.ultramic.2017.06.010.

Mirzayev, R., Mustonen, K., Monazam, M.R.A., Mittelberger, A., Pennycook, T.J., Mangler, C., Susi, T., Kotakoski, J., Meyer, J.C., 2017. Buckyball sandwiches. Sci. Adv. 3. https://doi.org/10.1126/sciadv.1700176.

Murata, K., Wolf, M., 2018. Cryo-electron microscopy for structural analysis of dynamic biological macromolecules. Biochim. Biophys. Acta - Gen. Subj. 1862, 324–334. https://doi.org/10.1016/j.bbagen.2017.07.020.

Plimpton, S., 1995. Fast parallel algorithms for short-range molecular dynamics. J. Comput. Phys. 117, 1–19. https://doi.org/10.1006/jcph.1995.1039.

Robertson, A.W., Warner, J.H., 2013. Atomic resolution imaging of graphene by transmission electron microscopy. Nanoscale 5, 4079. https://doi.org/10.1039/c3nr00934c.

Russo, C.J., Passmore, L.A., 2014. Ultrastable gold substrates for electron cryomicroscopy. Science 80 (346), 1377–1380. https://doi.org/10.1126/science.1259530.

Russo, C.J., Passmore, L.A., 2016. Ultrastable gold substrates: properties of a support for

high-resolution electron cryomicroscopy of biological specimens. J. Struct. Biol. 193, 33–44. https://doi.org/10.1016/j.jsb.2015.11.006.

Schneider, N.M., Norton, M.M., Mendel, B.J., Grogan, J.M., Ross, F.M., Bau, H.H., 2014. Electron–water interactions and implications for liquid cell electron microscopy. J. Phys. Chem. C 118, 22373–22382. https://doi.org/10.1021/jp507400n.

Siegel, G., 1972. Der Einfluß tiefer Temperaturen auf die Strahlenschädigung von organischen Kristallen durch 100 keV-Elektronen / The influence of very low temperature on the radiation damage of organic crystals irradiated by 100 keV-electrons. Zeitschrift für Naturforsch. A 27. https://doi.org/10.1515/zna-1972-0219.

Skowron, S.T., Chamberlain, T.W., Biskupek, J., Kaiser, U., Besley, E., Khlobystov, A.N., 2017. Chemical reactions of molecules promoted and simultaneously imaged by the electron beam in transmission electron microscopy. Acc. Chem. Res. 50, 1797–1807. https://doi.org/10.1021/acs.accounts.7b00078.

Smith, B.W., Monthioux, M., Luzzi, D.E., 1998. Encapsulated C60 in carbon nanotubes. Nature 396, 323–324. https://doi.org/10.1038/24521.

Stevens, A., Luzi, L., Yang, H., Kovarik, L., Mehdi, B.L., Liyu, A., Gehm, M.E., Browning, N.D., 2018. A sub-sampled approach to extremely low-dose STEM. Appl. Phys. Lett. 112, 043104. https://doi.org/10.1063/1.5016192.

Stuart, S.J., Tutein, A.B., Harrison, J.A., 2000. A reactive potential for hydrocarbons with intermolecular interactions. J. Chem. Phys. 112, 6472. https://doi.org/10.1063/1.481208.

Susi, T., Meyer, J.C., Kotakoski, J., 2017. Manipulating low-dimensional materials down to the level of single atoms with electron irradiation. Ultramicroscopy 180, 163–172. https://doi.org/10.1016/j.ultramic.2017.03.005.

Wei, X., Tang, D.-M., Chen, Q., Bando, Y., Golberg, D., 2013. Local coulomb explosion of boron nitride nanotubes under electron beam irradiation. ACS Nano 7, 3491–3497. https://doi.org/10.1021/nn400423y.

Wiktor, C., Meledina, M., Turner, S., Lebedev, O.I., Fischer, R.A., 2017. Transmission electron microscopy on metal–organic frameworks – a review. J. Mater. Chem. A 5, 14969–14989. https://doi.org/10.1039/C7TA00194K.

Wu, B., Neureuther, A.R., 2001. Energy deposition and transfer in electron-beam lithography. J. Vac. Sci. Technol. B Microelectron. Nanom. Struct. 19, 2508. https://doi.org/10.1116/1.1421548.

Zewail, A.H., Thomas, J.M., 2009. 4D Electron Microscopy: Imaging in Space and Time. Imperial College Press, London.

Zhao, X., Dan, J., Chen, J., Ding, Z., Zhou, W., Loh, K.P., Pennycook, S.J., 2018. Atom-by-atom fabrication of monolayer molybdenum membranes. Adv. Mater. 30, 1707281. https://doi.org/10.1002/adma.201707281.

Zubeltzu, J., Chuvilin, A., Corsetti, F., Zurutuza, A., Artacho, E., 2013. Knock-on damage in bilayer graphene: indications for a catalytic pathway. Phys. Rev. B 88, 245407. https://doi.org/10.1103/PhysRevB.88.245407.